

Improving Optoelectronic Properties of the 2,7-Polyfluorene Derivatives with Carbazole and Oxadiazole Pendants by Incorporating the Blue-Emitting Iridium Complex Pendants in C-9 Position of Fluorene Unit

Hua Tan, Junting Yu, Yafei Wang, Jianmin Li, Jiaojiao Cui, Jian Luo, Danyan Shi, Kai Chen, Yu Liu, Kaixuan Nie, Weiguo Zhu

Key Laboratory of Environment-Friendly Chemistry and Application in Ministry of Education, College of Chemistry, Xiangtan University, Xiangtan 411105, China

Correspondence to: W. Zhu (E-mail: zhuwg18@126.com) or Y. Liu (E-mail: liuyu03b@126.com)

Received 11 July 2011; accepted 12 September 2011; published online 11 October 2011

DOI: 10.1002/pola.25017

ABSTRACT: To study the influence of a blue-emitting iridium complex pendant on the optoelectronic properties of its 2,7-polyfluorene (PF) derivatives with the carbazole and oxadiazole pendants, a class of 2,7-PF derivatives containing carbazole, oxadiazole, and/or without the cyclometalated iridium complex pendants in the C-9 positions of fluorene unit were synthesized. Their thermal, photophysical, electrochemical, and electroluminescent (EL) properties were investigated. Among these 2,7-PF derivatives (P1–P4), P2 and P3 exhibited higher photoluminescence efficiency in dichloromethane and better EL properties in the single-emissive-layer polymer light-emitting devices. The highest brightness of 3888 cd/m² and the

maximum current efficiency of 2.9 cd/A were obtained in the P2- and P3-based devices, respectively. The maximum brightness and efficiency levels were 1.7 and 2.1 times, respectively, higher than the corresponding levels from the parent 2,7-PF derivative (P1)-based devices. Our work indicated that EL properties of 2,7-PF derivatives can be improved by introducing the blue-emitting iridium complex into the alkyl side chain of fluorene unit as pendant. © 2011 Wiley Periodicals, Inc. *J Polym Sci Part A: Polym Chem* 50: 149–155, 2012

KEYWORDS: conjugated polymers; iridium complex; 2,7-polyfluorene; light-emitting diodes (LED); metal-polymer complexes

INTRODUCTION 2,7-Polyfluorenes (PFs) and their derivatives as a class of the promising blue-emitting materials have attracted much interests, because they have high photoluminescence (PL) efficiencies both in solution and in solid films and can be substituted easily by various groups in C-9 position to tune the solubility and optoelectronic properties. To achieve high-efficiency polymer light-emitting diodes (PLEDs), various 2,7-PFs and their derivatives have been developed.^{1–4}

In general, 2,7-PF derivatives have high ionization potential, and there is a high-energy barrier between these 2,7-PF derivatives and electron-blocking layer of poly-(3,4-ethylenedioxythiophene) (PEDOT) that results in higher driving voltages and an unbalance in charge injection and transportation. Accordingly, various strategies have also been developed to overcome these deficiencies for PF derivatives.^{5–14} For example, Lin¹⁵ designed a series of the fluorene-based copolymers containing dendritic 1,3,4-oxadiazole pendants and obtained a PLED with a bright luminescence of 2446 cd/m² at 12 V and a current efficiency of 0.24 cd/A at 100 mA/cm². Peng et al.¹⁶

reported a class of the blue-emitting PF derivatives containing dendritic carbazole and oxadiazole pendants and presented a PLED with an improved emission color quality and an ascend-ant external quantum efficiency of 1.03%.

Recently, there was an increasing research activity in developing the fluorene-based copolymers as electrophosphorescent materials, because 2,7-PF derivatives have more advantages, and phosphorescent units have 100% internal quantum efficiency. In these developed phosphorescent fluorine-based copolymers, many red-emitting iridium (III) complex-based PF derivatives were studied and exhibited various electroluminescent (EL) properties. For example, Wang and coworkers¹⁷ synthesized a 2,7-PF derivative containing a pendent orange-emitting unit of iridium (III) bis(2-(4'-fluorophenyl)-4-phenylquinoline-N,C^{2'}) (tetradecane-dionate-11,13) in the C-9 position and obtained a white-emitting device with a maximum current efficiency of 4.49 cd/A and a Commission Internationale de l'Eclairage (CIE) coordinate of (0.46, 0.33) at 6.0 V. Cao reported a type of the fluorene-based copolymers, in which the iridium complex units with a

Additional Supporting Information may be found in the online version of this article.

© 2011 Wiley Periodicals, Inc.

cyclometalated ligand of 2-*p*-tolyl-benzothiazole were incorporated into the copolymers by either embedding or end-capping into the backbone. Their PLEDs exhibited a red emission peaked at 599 nm with a maximum external quantum efficiency of 2.19% at a current density of 0.3 mA/cm² and a maximum luminance of 2347 cd/m² at 17 V.¹⁸ Yang presented a series of 2,7-PF derivatives containing red-emitting iridium complexes and carrier-transporting units as the substitutes of the C-9 position of fluorene. A maximum current efficiency of 9.3 cd/A and a maximum power efficiency of 10.5 lm/W were obtained.¹⁹

However, there is few report on the PF derivatives attached the blue-emitting phosphorescent units onto the alkyl side chains of the PF. As PF has a triplet energy in the range of 2.1–2.3 eV which is lower than that of the blue-emitting iridium(III) bis[(4,6-difluorophenyl)pyridinato-N,C^{2'}] picolinate [Flr(pic)] (2.6 eV), the efficient energy transfer from Flr(pic) to PF is expected to occur.²⁰ Therefore, introducing a Flr(pic) unit onto the alkyl side chains of the PF derivatives should be a feasible strategy to improve the optoelectronic properties of its resulting PF derivatives due to the efficient energy transfer. To study the effect of the blue-emitting iridium complex unit on the optoelectronic properties of its PF derivatives, the Flr(pic) unit was introduced into PF derivatives containing the carbazole and oxadiazole pendants by an unconjugated linkage. The resulting 2,7-PF derivatives were synthesized, and the synthetic route is shown in Scheme 1. As expected, the PL and devices efficiency of these Flr(pic)-modified 2,7-PF derivatives were greatly improved when compared to the PF derivative without the Flr(pic) unit.

EXPERIMENTAL

Materials and Measurement

All manipulations were performed under dry nitrogen flow. All reagents were purchased from Aldrich and were directly used without further purification. The contents of the pendent Flr(pic) unit in PF derivatives are 2.5, 7.5, and 12.5 mol % for P2, P3, and P4, respectively. For comparison, P1 without the Flr(pic) pendant was synthesized at the same time. The intermediates of M1, M2, and 4-(5-(4-*tert*-butyl-phenyl)-1,3,4-oxadiazol-2-yl)phenol were synthesized according to the published procedures.^{4,21} M4 was synthesized based on our previous work.²²

¹H and ¹³C NMR spectra were recorded on a Bruker DRX 400 spectrometer by tetramethylsilane as a reference in deuterated chloroform solution at 298 K. MALDI-TOF mass spectrometric measurements were performed on Bruker Biflex III MALDI-TOF. Molecular weights for these PF derivatives were determined using a Waters GPC 2410 in tetrahydrofuran via a calibration curve of polystyrene as standard. UV absorption spectra were recorded with a HP-8453 UV-visible system. PL spectra were recorded on a HITACHI-850 fluorescence spectrophotometer. Cyclic voltammetry (CV) was performed on a CHI660A electrochemical work station in a solution of 0.1 M tetrabutylammonium hexafluorophosphate (Bu₄NPF₆) in acetonitrile at a scan rate of 100 mV/s and at room temperature (RT) under nitrogen protection. The PF

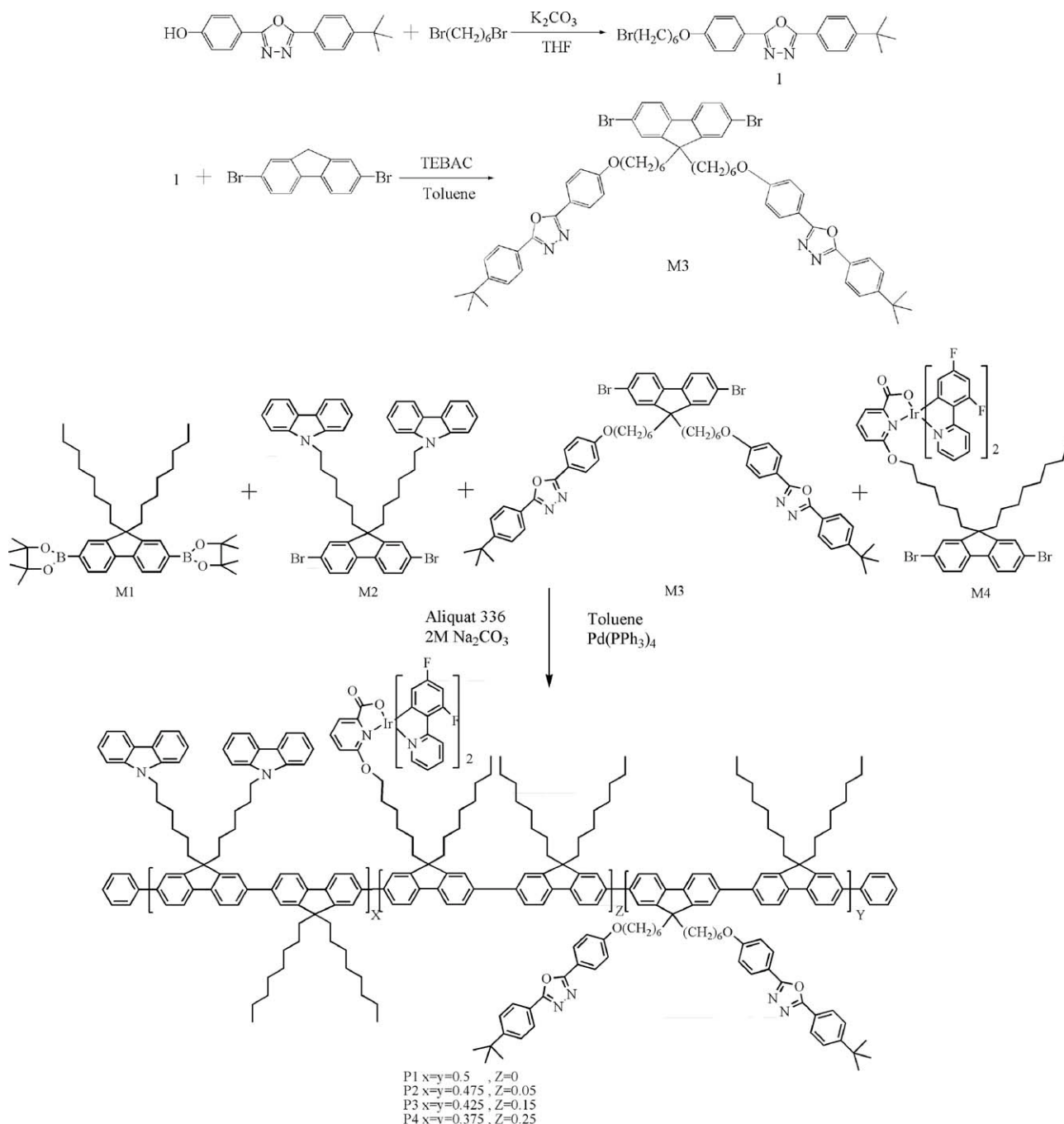
derivates were dissolved in the above solution (1 mg/cm³). A platinum rod and wire were used as a working electrode and a counter electrode, respectively. A calomel electrode was used as a reference electrode. Devices with a structure of indium tin oxide (ITO)/PEDOT (40 nm)/PVK (40 nm)/PF derivatives (80 nm)/CsF (4 nm)/Al (120 nm) were fabricated in a controlled dry-box (Vacuum Atmosphere) under N₂ circulation, where a poly(vinyl carbazole) (PVK) layer was used as a hole-transporting layer and a 4-nm thin layer of CsF with a 120-nm Al capping layer was used as cathode. The devices were fabricated by following a standard procedure. A 40-nm thick layer of PEDOT:poly(styrene sulfonic acid) was spun onto the precleaned ITO-glass substrates. Then, a 40-nm-thick layer of PVK was spun on the top of PEDOT. An 80-nm-thick emissive layer of the PF derivatives was spun on the top of PVK. A profilometer (Tencor Alfa-Step 500) was used to determine the thickness of the films. The current density (*J*)–voltage (*V*) data were collected using a Keithley 236 source measurement unit. Luminance was measured by a Si photodiode and calibrated by a PR-705 spectrascan spectrophotometer (Photo Research). EL spectra were recorded using a charged coupling device spectrophotometer (Instaspec 4, Oriel).

Synthesis of 2-(4-(6-Bromohexyloxy)phenyl)-5-(4-*tert*-butylphenyl)-1,3,4-oxadiazole (1)

A mixture of 4-(5-(4-*tert*-butylphenyl)-1,3,4-oxadiazol-2-yl)phenol (2.94 g, 10 mmol), 1,6-dibromohexane (14.7 g, 60.3 mmol), THF (50 mL), and K₂CO₃ (4.0 g, 40 mmol) were stirred vigorously under nitrogen protection at 70 °C for 24 h. The mixture was cooled to RT, poured into brine, and then extracted with dichloromethane (DCM). The combined organic layer was washed with brine for three times and dried over magnesium sulfate. After removal of the solvent, the excess 1,6-dibromohexane was separated from the mixture by vacuum distillation (130 °C/0.1 mmHg). The residue was purified by flash chromatography using hexane/DCM (V/V, 1:0–1:1) as eluent to give compound **1** (3.27 g, 71.6%) as white solid. ¹H NMR (CDCl₃, 400 MHz), δ (ppm): 1.33 (s, 9H), 1.53–1.58 (m, 8H), 1.93–1.95 (m, 4H), 3.45 (t, *J* = 6.8 Hz, 2H), 4.06 (t, *J* = 7.0 Hz, 2H), 7.02 (d, *J* = 8.2 Hz, 2H), 7.55 (d, *J* = 8.0 Hz, 2H), 8.03 (d, *J* = 8.0 Hz, 4H). ¹³C NMR (CDCl₃, 100 MHz), δ (ppm): 163.4, 163.24, 160.8, 154.1, 127.6, 125.8, 124.7, 120.4, 115.5, 114.0, 67.0, 34.0, 32.6, 31.7, 30.1, 28.0, 26.9, 24.1. TOF-MS (*m/z*): Calcd for C₂₄H₂₉BrN₂O₂, 456.1; found, 456.8.

Synthesis of M2

Compound **M2** was synthesized according to a synthetic procedure of compound **1**. Yield: 79%, mp: 80.0–80.4 °C. ¹H NMR (CDCl₃, 400 MHz), δ (ppm): 0.51–0.56 (m, 4H), 1.06–1.25 (m, 8H), 1.67–1.70 (m, 4H), 1.79–1.82 (m, 4H), 4.16 (t, *J* = 7.2 Hz, 4H), 7.18 (t, *J* = 7.6 Hz, 4H), 7.30–7.35 (m, 6H), 7.41–7.49 (m, 8H), 8.06 (d, *J* = 7.8 Hz, 4H). ¹³C NMR (CDCl₃, 100 MHz), δ (ppm): 152.2, 140.4, 139.0, 130.3, 126.1, 125.6, 122.8, 121.6, 121.2, 120.3, 118.7, 108.6, 55.5, 42.9, 40.0, 29.5, 28.7, 26.8, 23.5. TOF-MS (*m/z*): Calcd for C₄₉H₄₆Br₂N₂, 822.7; found, 822.1.



SCHEME 1 Synthetic route of the PF derivatives containing carbazole, oxadiazole, and iridium complex pendants.

Synthesis of M3

A mixture of 2,7-dibromo-9H-fluorene (3.24 g, 10 mmol), compound **1** (9.14 g, 20 mmol), aqueous sodium hydroxide (33%, 20 mL), toluene (50 mL), and tetrabutyl ammonium bromide (0.1 g) were stirred vigorously under nitrogen protection for 24 h at 80 °C. The mixture was cooled to RT and extracted with DCM (3 × 50 mL). The combined organic layer was dried over magnesium sulfate and evaporated under reduced pressure to remove toluene. The residue was purified by flash chromatography using ethyl acetate/DCM (V/V, 1:10)

as eluent to give compound **M3** as white solid (8.37 g, 77.8 %), mp: 120.8–121.1 °C. $^1\text{H NMR}$ (CDCl_3 , 400 MHz), δ (ppm): 0.64–0.67 (br, 4H), 1.14–1.37 (m, 30H), 1.60–1.66 (m, 4H), 1.94–1.98 (m, 4H), 3.91 (t, $J = 4.0$ Hz, 4H), 6.96 (d, $J = 6.0$ Hz, 4H), 7.44–7.47 (m, 4H), 7.48 (t, $J = 8.0$ Hz, 2H), 7.52–7.55 (m, 4H), 8.00 (d, $J = 7.0$ Hz, 8H). $^{13}\text{C NMR}$ (CDCl_3 , 100 MHz), δ (ppm): 164.4, 164.2, 161.9, 155.2, 152.3, 139.1, 130.4, 128.6, 126.7, 126.1, 126.0, 121.6, 121.2, 116.2, 115.0, 68.1, 55.6, 40.1, 35.1, 31.1, 29.5, 28.9, 25.6, 23.6. TOF-MS (m/z): Calcd for $\text{C}_{61}\text{H}_{64}\text{Br}_2\text{N}_4\text{O}_4$, 1076.3; found, 1077.3.

TABLE 1 Polymerization Results and Thermal Properties of the PF Derivatives

	Polymer	M_n^a	M_w^a	Polydispersity index ^a	T_d^b (°C)	T_g^c (°C)
1	P1	20,365	33,892	1.66	416	93
2	P2	12,136	20,025	1.65	417	94
3	P3	9,285	17,019	1.83	367	79
4	P4	22,092	54,704	2.47	397	105

^a M_n , M_w , and polydispersity index of the polymers were determined by gel permeation chromatography using polystyrene standards.

^b T_d were measured by TGA at a temperature of 5% weight loss.

^c T_g were determined by DSC.

General Procedures of Suzuki Polycondensation, Taking P2 For Example

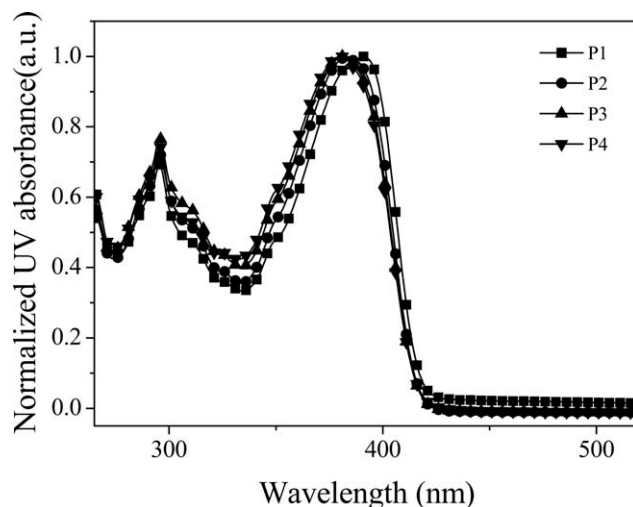
Tetrakis(triphenylphosphine)palladium (10 mg) was added under a nitrogen atmosphere into a degassed mixture containing the monomers M1 (128.5 mg, 0.2 mmol), M2 (78.16 mg, 0.095 mmol), M3 (102.2 mg, 0.095 mmol), and M4 (12.29 mg, 0.01 mmol), Na₂CO₃ aqueous solution (2.0 M, 2.0 mL), and Aliquat 336 (two drops) in toluene (4 mL). The mixture was stirred vigorously and heated at 90 °C for 48 h. The end groups were capped by heating the resulting mixture under reflux for 12 h with 2,4-difluorobenzeneboronic acid (31.4 mg, 0.200 mmol) and for another 12 h with bromobenzene (34 mg, 0.220 mmol). The mixture was then cooled to RT and dropped into 200 mL MeOH to form precipitate. The precipitate was collected and dissolved in DCM. The resulting DCM solution was dropped into 200 mL MeOH again to obtain precipitate. This new precipitate was washed with acetone under refluxing for 48 h in a Soxhlet apparatus and dried under vacuum to give P2 (105 mg, 28 %) as a yellowish solid. ¹H NMR (CDCl₃, 400 MHz), δ (ppm): 0.56–1.45 (m, 68 H), 1.47–1.82 (br, 8H), 1.88–2.31 (br, 16H), 3.83–3.95 (m, 4H), 4.06–4.23 (br, 4H), 6.83–7.04 (m, 4H), 7.09–7.23 (m, 4H), 7.26–7.92 (m, 36H), 7.94–8.16 (m, 12H). ¹³C NMR (CDCl₃, 100 MHz), δ (ppm): 164.4, 164.2, 161.9, 155.1, 151.8, 151.4, 140.4, 140.1, 132.2, 128.6, 126.7, 126.0, 125.5, 122.8, 121.8, 120.3, 118.7, 116.4, 114.9, 108.6, 68.1, 55.4, 42.9, 40.4, 35.1, 32.0, 31.8, 31.2, 30.0, 29.8, 29.7, 29.2, 29.0, 28.8, 26.9, 26.3, 25.9, 25.6, 23.9, 22.7, 22.6, 14.1.

TABLE 2 Absorption, Emission Properties of the PF Derivatives

Polymer	Absorption ^a λ /nm ($\epsilon_{\max}/\text{dm}^3 \text{ mol}^{-1} \text{ cm}^{-1}$)	Emission (measured in CH ₂ Cl ₂ at 298 K) λ_{\max} (nm)	Emission (measured in the neat film at 298 K) λ_{\max} (nm)	Φ_f^b
P1	294(6.8 × 10 ⁵), 390(8.8 × 10 ⁵)	417, 440	449, 526	0.41
P2	296(8.1 × 10 ⁵), 383(5.7 × 10 ⁵)	417, 439	447, 527	0.68
P3	296(6.3 × 10 ⁵), 381(7.9 × 10 ⁵)	417, 438	450, 536	0.77
P4	296(5.6 × 10 ⁵), 381(5.6 × 10 ⁵)	417, 438	449, 536	0.62

^a Measured in CH₂Cl₂ at a concentration of 10⁻⁶ mol/L.

^b Measured in CH₂Cl₂ at 298 K. Excitation wavelength was 380 nm, and 9,10-diphenylanthracene ($\Phi_f = 0.9$) was used as the reference.

**FIGURE 1** Normalized UV-vis absorption spectra of the PF derivatives in DCM at RT.

P1, 131 mg, yellowish solid. Yield: 42%. ¹H NMR (CDCl₃, 400 MHz), δ (ppm): 0.59–1.45 (m, 68 H), 1.46–1.86 (m, 8H), 1.93–2.45 (br, 16H), 3.79–4.00 (m, 4H), 4.06–4.25 (br, 4H), 6.85–7.00 (m, 4H), 7.16–7.21 (m, 4H), 7.21–7.92 (m, 36H), 7.93–8.15 (m, 12H). ¹³C NMR (CDCl₃, 100 MHz), δ (ppm): 164.4, 164.2, 161.9, 155.1, 151.8, 140.4, 128.6, 126.7, 126.0, 125.5, 122.8, 121.4, 120.3, 118.7, 115.0, 114.9, 108.6, 68.1, 55.4, 42.9, 40.4, 35.1, 31.8, 31.1, 30.0, 29.7, 29.1, 25.6, 23.9, 22.6, 14.1.

P3, 85 mg, yellowish solid. Yield: 26%. ¹H NMR (CDCl₃, 400 MHz), δ (ppm): 0.63–1.46 (m, 68 H), 1.48–1.77 (m, 8H), 1.91–2.33 (br, 16H), 3.84–3.96 (m, 4H), 4.07–4.24 (br, 4H), 6.84–6.99 (m, 4H), 7.10–7.25 (m, 4H), 7.27–7.91 (m, 36H), 7.96–8.14 (m, 12H). ¹³C NMR (CDCl₃, 100 MHz), δ (ppm): 164.4, 161.9, 155.1, 151.9, 140.4, 140.1, 128.8, 127.2, 126.7, 126.0, 125.5, 122.8, 121.4, 120.3, 120, 118.7, 116.4, 114.9, 108.6, 68.1, 55.4, 42.9, 40.4, 35.1, 31.8, 31.2, 30, 29.7, 29.2, 29, 28.8, 26.9, 25.7, 23.9, 22.6, 14.1.

P4, 65 mg, yellowish solid. Yield: 20%. ¹H NMR (CDCl₃, 400 MHz), δ (ppm): 0.64–1.42 (m, 68 H), 1.42–1.79 (m, 8H), 1.93–2.23 (br, 16H), 3.81–3.96 (m, 4H), 4.07–4.27 (br, 4H), 6.89–6.98 (m, 4H), 7.11–7.25 (m, 4H), 7.27–7.91 (m, 36H), 7.94–8.12 (m, 12H). ¹³C NMR (CDCl₃, 100 MHz), δ (ppm): 164.4, 164.2, 161.9, 155.1, 151.8, 140.4, 140.1, 128.6, 126.7,

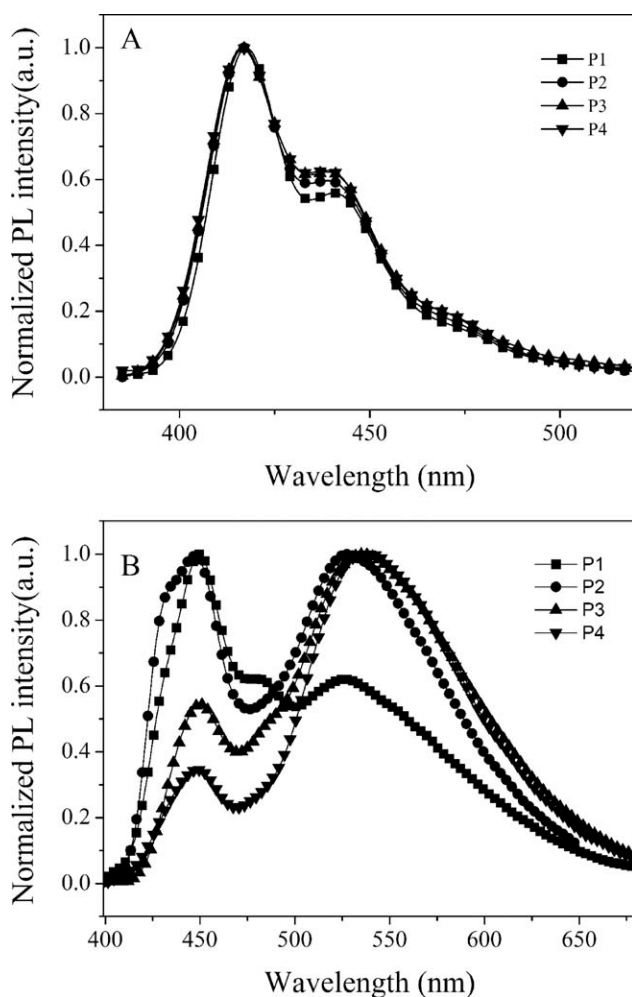


FIGURE 2 Normalized PL spectra of the PF derivatives in DCM (A) and their neat films (B) at RT.

126.1, 126.0, 125.5, 122.8, 121.3, 120.3, 120, 118.6, 116.4, 114.9, 108.6, 68.2, 55.4, 42.9, 40.4, 35.1, 31.8, 31.2, 30, 29.7, 29.2, 29, 28.8, 26.9, 25.7, 23.9, 22.6, 14.0.

RESULTS AND DISCUSSION

Thermal Property

The thermal property of these PF derivatives of P1, P2, P3, and P4 were determined by differential scanning calorimeter

(DSC) and thermogravimetry analysis (TGA). Their glass transition temperatures (T_g) and thermal degradation temperatures (T_d) for 5% weight loss are listed in Table 1. The corresponding TGA and DSC curves are shown in Figures S1 and S2, Supporting Information. Obviously, these PF derivatives exhibit high T_g and T_d , in which T_g varies from 79 to 105 °C and T_d is over 367 °C. Compared to poly(9,9-dihexylfluorene) ($T_g = 55$ °C), these PF derivatives containing carbazole, oxadiazole, and iridium complex pendants present higher T_g . Therefore, incorporating the pendants of carbazole, oxadiazole and iridium complex into the alkyl side chain of PF can improve the thermal stabilities of their 2,7-PF derivatives.

Optical Properties

The UV-vis absorption spectra of these PF derivatives in dilute DCM are shown in Figure 1, and their data are summarized in Table 2. Almost similar UV-vis absorption spectra are displayed in these PF derivatives of P1–P4. Two typical and intense absorption bands are observed at about 300 nm and 381 nm, respectively. The first high-lying one is attributed to the π - π^* transitions from the pendants of carbazole, oxadiazole, and iridium complex. The second low-lying one is assigned to the π - π^* transition associated with the PF backbone. However, the metal-ligand charge transfer absorption from the iridium complex unit is very hard to observe owing to the influence of much strong π - π^* transition absorption of the pendants and PF backbone. This phenomenon is also formed in the red-emitting phosphorescent PF derivatives.²³

The PL spectra of these PF derivatives in dilute DCM and in their neat thin films are shown in Figure 2, as well as their data are also summarized in Table 2. Almost identical PL profiles with stable and strong purple-blue emission are also exhibited for all of these PF derivatives in dilute DCM. The maximum emissive peak at 417 nm and a shoulder at 438 nm are observed, which is a characteristic emission of poly(9,9-dioctylfluorene) (PFO) backbone. Emissions from the pendants of the carbazole, oxadiazole, and iridium complex are not significantly displayed. This implies that efficient energy transfer from these pendants to the polymer backbone has occurred. We note that the PL quantum yields of the P1, P2, P3, and P4 in DCM were measured to be 0.41, 0.68, 0.77, and 0.62, respectively, using 9,10-diphenylanthracene ($\Phi_f = 0.9$) as reference. Therefore, attaching the

TABLE 3 Electrochemical Properties of the Polyfluorene Derivatives

Polymer	$E_{1/2}^{ox}$ (V)	$E_{1/2}^{red}$ (V)	E_{HOMO}^b (eV)	E_{LUMO}^c (eV)	E_g^c (eV)	E_{opt}^d (eV)
P1	1.62	-1.65	-5.96	-2.69	3.27	2.95
P2	1.60	-1.79	-5.94	-2.55	3.39	2.95
P3	1.60	-1.71	-5.94	-2.63	3.31	2.95
P4	1.56	-1.72	-5.90	-2.62	3.28	2.94

^a Potential values are reported by cyclic voltammetry versus Fe/Fe⁺.

^b $E_{HOMO} = -(4.34 + E_{1/2}^{ox})$ eV.

^c $E_{LUMO} = -(4.34 + E_{1/2}^{red})$ eV, $E_g = E_{LUMO} - E_{HOMO}$.

^d Estimated according to the UV-vis absorption spectrum.

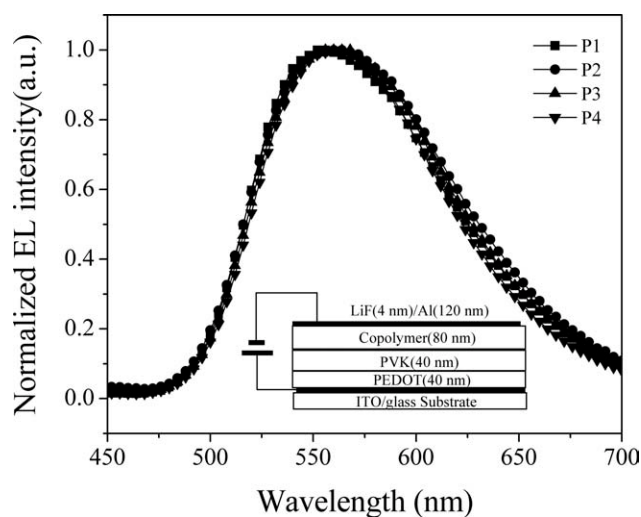


FIGURE 3 EL spectra for the PF derivative-based PLEDs.

blue-emitting FIr(pic) pendant onto the alkyl side-chain of the PF derivatives is available to improve the emission quantum efficiency of its resulting PF derivatives.

However, these PF derivatives in the neat thin films exhibited significantly different PL spectra instead of in dilute DCM. Two typical emission bands were observed at around 449 and 530 nm, in which the high-lying emission band comes from the fluorene-based backbone, and the low-lying emission band is attributed to excimer emission of these PF derivatives.⁴ As this kind of PF derivatives contains the oxadiazole unit with an accepting electron effect and carbazole unit with a donating electron effect, there is a donor-acceptor effect in them, the PF derivatives are available to exhibit intense excimer emission.^{24,25} In addition, the P2, P3, and P4 presented much stronger excimer emission than the P1 under photoexcitation. This indicates that the incorporated blue-emitting FIr(pic) unit with an accepting electron effect can facilitate the molecular donor-acceptor effect in

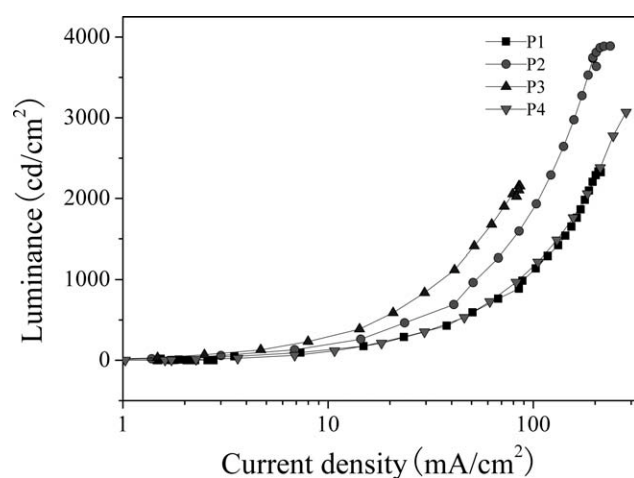


FIGURE 4 Current density-luminance characteristics of the PF derivative-based PLEDs.

TABLE 4 Device Performances of the Polyfluorene Derivative-Based PLEDs

Polymer	$V_{\text{turn-on}}$ (V)	L_{max} (cd/m ²)	LE (cd/A)	λ_{max} (nm)	CIE
P1	5.6	2,334	1.35	556	0.41, 0.55
P2	6.0	3,888	1.97	561	0.40, 0.54
P3	7.2	2,153	2.90	560	0.42, 0.54
P4	8.7	3,068	1.19	558	0.44, 0.52

the solid state and result in enhanced excimer emission of its PF derivatives under photoexcitation.

Electrochemical Property

The redox behaviors of these PF derivatives in the neat films were studied by CV using an anhydrous electrolyte of 0.1 M tetrabutylammonium hexafluorophosphate (Bu_4NPF_6) in CH_3CN solution. All of these polymers presented a reversible oxidation potential (E^{ox}) at about 1.56–1.61 V and a reversible reduction potential (E^{red}) at about –1.65 to –1.79 V. The E^{red} and E^{ox} data are listed in Table 3. It is obvious that the FIr(pic)-modified polyfluorene derivatives (P2–P4) show lower oxidation and reduction potentials than the P1 copolymer. To further study the influence of the blue-emitting FIr(pic) pendant on the energy levels of its PF derivatives, the highest occupied molecular orbital (HOMO) and the lowest unoccupied molecular orbital (LUMO) energy levels (E_{HOMO} and E_{LUMO}) were calculated based on the following empirical formula: $E_{\text{HOMO}} = -(E^{\text{ox}} + 4.34)$ eV and $E_{\text{LUMO}} = -(E^{\text{red}} + 4.34)$ eV. The results show that the HOMO and LUMO energy levels of these PF derivatives are around –5.93 eV and –2.62 eV, respectively. Although the optical band gaps (E_{opt}) are identical for these copolymers, the FIr(pic)-modified PF derivatives (P2–P4) present higher E_{HOMO} and E_{LUMO} than P1. This means that incorporating the blue-emitting FIr(pic) unit into alkyl side chain of PF is in favor of promoting the HOMO and LUMO energy levels; thus, the energy barrier of charge injection from anode to emitters is decreased.

Electroluminescence Properties

The EL spectra from these PF derivative-based PLEDs are shown in Figure 3. Almost identical EL spectra with a maximum emission peak around 560 nm are observed in these devices. No emission from the PF backbone and the pendants of carbazole, oxadiazole, and iridium complex was observed. Compared to the PL spectra in the neat films, the EL may be attributed to the excimer emission of these PF derivatives.²⁰ It is suggested that the donor-acceptor effect in these PF derivatives plays a much important role in the excimer formation and emission under electric field.²⁴ Unlike the significantly changed PL spectra in the neat films, the EL spectra have little change with increasing FIr(pic) units for these PF derivatives. This indicates that incorporating blue-emitting FIr(pic) onto alkyl side chain of PF derivatives has little influence on excimer emission of its PF derivatives under electric field.

The current density-voltage-luminance curves of these PF derivative-based PLEDs are shown in Figure 4, and the device performances are summarized in Table 4. The turn-on

voltage is observed to increase with increasing Flr(pic) units which is considered to be related to the carrier-trapped effect of these PF derivatives. On the other hand, the blue-emitting Flr(pic)-modified PF derivatives (P2,P3) exhibit higher current efficiency than the P1 in the devices. With increasing Flr(pic) units from 0 to 7.5 mol %, the PF derivatives exhibited an increased current efficiency in the devices. However, with further increasing Flr(pic) units from 7.5 to 12.5 mol %, the PF derivatives displayed a decreased current efficiency. Among these PF derivatives, P3 displays a highest current efficiency of 2.90 cd/A at 232 mA/cm², and P2 exhibits a highest brightness of 3888 cd/m² at 237 mA/cm² in the devices. The brightness and current efficiency levels are 1.7 and 2.1 times higher than the corresponding levels of the P1-based devices, respectively. This indicates that incorporating the blue-emitting Flr(pic) units with proper ratios into alkyl side chain of PF is available to improve the EL performance of its PF derivatives containing carbazole and oxadiazole units in the PLEDs.

CONCLUSIONS

We obtained a series of the PF derivatives grafted with oxadiazole, carbazole, and/without the blue-emitting cyclometalated iridium complex in the alkyl side chain units. Among these copolymers, the iridium complex modified PF derivatives exhibit higher PL efficiencies in DCM and better device performance in the PLEDs. A maximum brightness of 3888 cd/m² and a maximum current efficiency of 2.90 cd/A were achieved in the P2- and P3-based devices, respectively. The EL performance of the PF derivatives was significantly improved by incorporating a blue-emitting iridium complex into alkyl side chain of fluorine as pendant.

The authors thank the financial support from the National Natural Science Foundation of China (50973093, 20872124, and 20772101), the Specialized Research Fund and the New Teachers Fund for the Doctoral Program of Higher Education (20094301110004 and 200805301013), the Scientific Research Fund of Hunan Provincial Education Department (10A119, 11CY023, and 10B112), the Science Foundation of Hunan Province (2009FJ2002), and the Postgraduate Science Foundation for Innovation in Hunan Province (CX2011B263).

REFERENCES AND NOTES

1 Zhuang, X. D.; Chen, Y.; Li, B. X.; Ma, D. G.; Zhang, B.; Li, Y. X. *Chem Mater* 2010, 22, 4455–4461.
 2 Huang, W. S.; Wu, Y. H.; Hsu, Y. C.; Lin, H. C.; Lin, J. T. *Polymer* 2009, 50, 5945–5958.

3 Wu, F. I.; Shih, P. I.; Shu, C. F. *Macromolecules* 2005, 38, 9028–9036.
 4 Sung, H. H.; Lin, H. C. *J Polym Sci A: Polym Chem* 2005, 43, 2700–2711.
 5 Montilla, F.; Mallavia, R. *Adv Funct Mater* 2007, 17, 71–78.
 6 Kulkarni, A. P.; Kong, X.; Jenekhe, S. A. *J Phys Chem B* 2004, 108, 8689–8701.
 7 Jin, Y.; Kim, J. Y.; Park, S. H.; Kim, J.; Lee, S.; Lee, K.; Suh, H. *Polymer* 2005, 46, 12158–12165.
 8 Shu, C. F.; Dodda, R.; Wu, F. I. *Macromolecules* 2003, 36, 6698–6703.
 9 Liu, M. S.; Jiang, X.; Liu, S.; Herguth, P.; Jen, A. K.-Y. *Macromolecules* 2002, 35, 3532–3538.
 10 Lin, Y.; Chen, Y.; Chen, Z.; Ma, D.; Zhang, B.; Ye, T.; Da, Y. *Eur Polym J* 2010, 46, 997–1003.
 11 Assaka, A. M.; Rodrigues, P. C.; Oliveira, R.-M.; Ding, L.; Karasz, F. E.; Akcelrud, L. *Polymer* 2004, 45, 7071–7081.
 12 Kulkarni, A. P.; Zhu, Y.; Jenekhe, S. A. *Macromolecules* 2005, 38, 1553–1563.
 13 Lee, J. K.; Fong, H. H.; Zakhidov, A. A.; McCluskey, G. E.; Taylor, P. G.; Ober, C. K. *Macromolecules* 2010, 43, 1195–1198.
 14 Lindgren, L.; Wang, J. X.; Andersson, M. R. *Synth Met* 2005, 154, 97–100.
 15 Wu, C.-W.; Tsai, C.-M.; Lin, H.-C. *Macromolecules* 2006, 39, 4298–4305.
 16 Peng, Q.; Xu, J.; Li, M.; Zheng, W. *Macromolecules* 2009, 42, 5478–5485.
 17 Mei, C. Y.; Ding, J. Q.; Yao, B.; Cheng, Y. X.; Xie, Z. Y.; Geng, Y. H.; Wang, L. X. *J Polym Sci A: Polym Chem* 2007, 45, 1746–1757.
 18 Zhang, K.; Chen, Z.; Yang, C. L.; Zou, Y.; Qin, J. G.; Cao, Y. *J Mater Chem* 2008, 18, 3366–3375.
 19 Yang, X. H.; Wu, F.-I.; Neher, D.; Chien, C. H.; Shu, C. F. *Chem Mater* 2008, 20, 1629–1635.
 20 Ma, Z. H.; Ding, J. Q.; Zhang, B. H.; Mei, C. Y.; Cheng, Y. X.; Xie, Z. Y.; Wang, L. X.; Jing, X. B.; Wang, F. S. *Adv Funct Mater* 2010, 20, 138–146.
 21 Wang, Y. F.; Tan, H.; Liu, Y.; Hu, Z. Y.; Zhu, M. X.; Wang, L.; Zhu, W. G.; Cao, Y. *Tetrahedron* 2010, 66, 1483–1488.
 22 Wang, Y. F.; Liu, Y.; Zhang, Z. Y.; Luo, J.; Shi, D. Y.; Tan, H.; Lei, G. T.; Zhu, M. X.; Zhu, W. G.; Cao, Y. *Dyes Pigments* 2011, 91, 495–500.
 23 Tan, H.; Yu, J. T.; Nie, K. X.; Chen, J. H.; Deng, X. P.; Zhang, Z. Y.; Lei, G. T.; Zhu, M. X.; Liu, Y.; Zhu, W. G. *Polymers* 2011, 52, 4792–4797.
 24 Jin, Y.; Song, S.; Kim, J. Y.; Kim, H.; Lee, K.; Suh, H. *Thin Solid Films* 2008, 516, 7373–7380.
 25 Yamada, H.; Park, S. H.; Song, S.; Heo, M.; Shim, J. Y.; Jin, Y.; Lee, H.; Lee, K.; Yoshinaga, K.; Kim, J. Y.; Suh, H. *Polymer* 2010, 51, 6174–6181.